Dual-Specific Cdc25B Phosphatase: In Search of the Catalytic Acid†

Wen Chen, Manuel Wilborn, and Johannes Rudolph*

Department of Biochemistry, Duke University Medical Center, Durham, North Carolina 27710

Received April 20, 2000; Revised Manuscript Received June 19, 2000

ABSTRACT: Cdc25 is a dual-specificity phosphatase that catalyzes the activation of the cyclin-dependent kinases, thus causing initiation and progression of successive phases of the cell cycle. Although it is not significantly structurally homologous to other well-characterized members, Cdc25 belongs to the class of well-studied cysteine phosphatases as it contains their active site signature motif. However, the catalytic acid needed for protonation of the leaving group has yet to be identified. To elucidate the role and identity of this key catalytic residue, we have performed a detailed pH-dependent kinetic analysis of Cdc25B. The pK_a of the catalytic cysteine was found to be 5.6−6.3 in steady state and one-turnover burst experiments using the small molecule substrates *p*-nitrophenyl phosphate and 3-*O*-methylfluorescein phosphate. Interestingly, Cdc25B does not exhibit the typical bell-shaped pH−rate profile with small molecule substrates seen in other cysteine phosphatases and indicative of the catalytic acid because it lacks pH dependence between 6.5 and 9. Reactions of Cdc25B with the natural substrate Cdk2-pTpY/CycA, however, did yield a bell-shaped pH−rate profile with a pK_a of 6.1 for the catalytic acid residue. Recent structural studies of Cdc25 have suggested that Glu474 [Fauman, E. B., et al. (1998) *Cell 93*, 617−625] or Glu478 [Reynolds, R. A., et al. (1999) *J. Mol. Biol. 293*, 559−568] could function as the catalytic acid in Cdc25B. Using site-directed mutagenesis and truncation experiments, however, we found that neither of these residues, nor the unstructured C-terminus, is responsible for the observed pH dependence. These results indicate that the catalytic acid does not appear to lie within the known structure of Cdc25B and may lie on its protein substrate.

Protein phosphorylation as mediated by protein kinases and phosphatases is a ubiquitous and essential element of signal transduction and cellular regulation. Protein phosphatases fall into two general classes (*1*). The serine/threonine phosphatases proceed via a one-step mechanism and are dependent on metal ions (i.e., Mn^{2+}, Fe^{2+}, and Zn^{2+}) for activity. The protein tyrosine phosphatases (PTPs)[1] proceed via a two-step mechanism that involves formation of a phosphocysteine intermediate. The PTPs are characterized by the active site sequence motif HCX_5R, where H is a highly conserved histidine residue, C is the catalytic cysteine, the five X residues form a loop, and R is a highly conserved arginine. There exists a subclass of the PTPs, termed the dual-specificity phosphatases (DSPs). Members of this subclass contain the conserved HCX_5R motif, are not significantly structurally homologous to the PTPs outside of this active site motif, and are able to hydrolyze phosphoserine/threonine as well as phosphotyrosine residues. An important member of the DSP family is the Cdc25 phosphatase (*2*). Cdc25 dephosphorylates the phosphothreonine (pT) and phosphotyrosine (pY) residues located in the Gly rich loop of the cyclin-dependent kinases (Cdks). Cdc25-mediated dephosphorylation of the Cdks leads to their activation and, thus, initiation and progression of successive phases of the cell cycle. Three homologues of Cdc25 exist in humans, Cdc25A, -B, and -C. The Cdc25 proteins are approximately 500 amino acids long (for a sequence alignment, see ref *3*). The N-termini have a low degree of sequence homology (level of identity of 20−25%) and contain numerous phosphorylation sites as well as nuclear import and/or export signals. The catalytic cores, including the HCX_5R motif, are located in the more homologous C-termini (∼60% identical over 200 amino acids).

Many detailed enzymological and structural studies of representative DSPs and PTPs have contributed to a detailed understanding of the mechanism of phosphatases containing the HCX_5R motif (Scheme 1) (for reviews, see refs *1* and *4*). The phosphorylated substrate binds in an active site containing an unprotonated thiolate and a protonated aspartic acid (*5*, *6*). The dianionic phosphate is cradled by the active site loop, forming hydrogen bonds to the backbone amides of the HCX_5R motif and to the guanidinium group of the arginine side chain of the HCX_5R motif (*7*). The thiolate anion of the active site cysteine lies directly below the phosphoryl group and is partially activated by an H-bond to a serine (*8*). This sets up an in-line attack of the thiolate on the P−O bond, leading to a phosphocysteine intermediate and efficient expulsion of the leaving group. The aspartic acid, which is located on a separate loop near the top of the active site cleft, assists in cleavage of the P−O bond by

† This work was supported by start-up funding from the Department of Biochemistry, Duke University Medical Center.

* To whom correspondence should be addressed. Phone: (919) 668-6188. Fax: (919) 613-8642. E-mail: rudolph@biochem.duke.edu.

[1] Abbreviations: PTPs, protein tyrosine phosphatases; DSPs, dual-specific phosphatases; Cdk, cyclin-dependent kinase; Cyc, cyclin; mFP, 3-*O*-methylfluorescein phosphate; pNPP, *p*-nitrophenyl phosphate; pT, phosphothreonine; pY, phosphotyrosine; Δ25B1, catalytic domain of Cdc25B (residues 377−549); Δ25B2, catalytic domain of Cdc25B (residues 377−566).

10.1021/bi000909u CCC: $19.00
Published on Web 08/11/2000

Scheme 1: Proposed Catalytic Mechanism of Cdc25

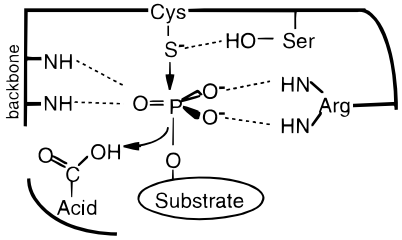

protonating the leaving group (*9*, *10*). The loop containing this catalytic acid has been shown to exist in several different conformations (*7*, *11*, *12*). In the open conformation when there is no substrate bound, the loop is flipped up and away from the active site, moving the aspartic acid 8−12 Å from the position it adopts upon binding of the phosphorylated substrate. The catalytic cycle is completed by the hydrolysis of the phosphocysteine intermediate, which requires deprotonation of the nucleophilic water molecule by a general base. There is mutagenic and structural evidence suggesting that the same aspartic acid residue that was the catalytic acid in the formation of the phosphocysteine intermediate plays the role of the catalytic base in the hydrolysis of this intermediate (*13*). Thus, the cysteine nucleophile and the catalytic acid are key residues in the reaction cycle of the DSPs and PTPs.

Despite the sequence diversity among the various phosphatases containing the HCX_5R motif, all structurally characterized PTPs and DSPs, except for Cdc25, share a common architecture. They all contain a central, highly twisted β-sheet with four central parallel β-strands flanked by five antiparallel β-strands, and this sheet is surrounded by six α-helices. The two important catalytic residues, the nucleophilic cysteine and the catalytic acid, have been identified in all of these enzymes, except for Cdc25, by structural studies, mutagenesis, and/or sequence alignments. In vaccinia H1-related phosphatase (VHR), the archetypical member of the DSP family, Cys124 is the catalytic cysteine of the HCX_5R motif and Asp92 is the catalytic acid (*14*−*16*). In the *Yersinia* phosphatase, Cys403 and Asp356 have been identified as the critical residues (*8*, *9*, *11*), whereas Cys293 and Asp262 have been found to be the key residues in the mitogen-activated protein kinase phosphatase (MKP3).

Recently, the structures of the catalytic domains of two of the three isoforms of Cdc25 have been determined (*17*, *18*). A 189-amino acid segment of the catalytic domain of Cdc25A was crystallized, and despite attempts to obtain a complete picture, the structure lacks a bound substrate and is disordered in the last 31 residues. A 211-amino acid segment of the catalytic domain of Cdc25B was crystallized with various oxyanions (sulfate and tungstate) bound in the active site with the disordered region at the C-terminus limited to the last 18 residues. As predicted by homology modeling (*19*), Cdc25A and Cdc25B catalytic domains form a small α/β-domain with a central five-stranded parallel β-sheet sandwiched by three α-helices from below and two α-helices from above. This topology is identical to that of the sulfur transfer protein rhodanese, a highly conserved protein in bacteria and mitochondria whose exact function is unknown. The HCX_5R forms the active site loop, with Cys473 (in Cdc25B) being the catalytic cysteine. Interestingly, neither of the two structure determinations exhibits a loop overhanging the active site that contains the putative catalytic acid, and no similar sequence motif can be detected by sequence comparisons. Earlier homology modeling and mutagenesis experiments identified Asp383 in Cdc25A as the potential catalytic acid (*20*). However, the crystal structures show that Asp383 points away from the active site and forms a buried and structurally important salt bridge with Arg385. On the basis of the crystal structure of Cdc25A, the Saper laboratory has suggested that Glu431, the first of the X residues in the HCX_5R signature motif, could serve the role of the elusive catalytic acid. In the structure of Cdc25B, on the other hand, Glu474 (corresponding to Glu431 in Cdc25A) is held away from the phosphate-binding region by hydrogen bonds to the OH group of Tyr528 and the NH group of Met531 and a water bridge to the apical oxygen atom of the bound sulfate. These authors therefore suggest that Glu478 (corresponding to Glu435 in Cdc25A), the last of the X residues in the HCX_5R motif, is the more likely candidate for the catalytic acid. A third possibility for the location of the catalytic acid is within the unstructured C-terminus, which could fold over the active site, thus mimicking the loop movement known from other DSPs and PTPs. Within this C-terminal region, there are two glutamates that are conserved in all three human Cdc25s and that could function as the catalytic acids, Glu553 and Glu558 in Cdc25B (corresponding to Glu510 and Glu515 in Cdc25A).

In this paper, we have performed a detailed pH-dependent kinetic analysis of the Cdc25B phosphatase using the artificial substrates pNPP and mFP and the natural substrate Cdk2-pTpY/CycA. In these studies, we have addressed the pK_as of the substrate and the catalytic cysteine and have investigated the possibility that Glu474, Glu478, or some unknown residue in the C-terminal region could play the role of the catalytic acid. Although the catalytic mechanism of Cdc25B appears to parallel that seen for other members of the DSP family, requiring the presence of a catalytic acid, the identity of this residue remains elusive.

EXPERIMENTAL PROCEDURES

Reagents. *p*-Nitrophenyl phosphate (pNPP) and 3-*O*-methylfluorescein phosphate (mFP) were purchased from Sigma. The pET3a vector and Pfu polymerase were purchased from Stratagene. The pGEX4T-1 vector, [γ-^{32}P]ATP, SP-Sepharose, and S-200 Superdex chromatography resins were obtained from Amersham-Pharmacia. All other reagents were of the highest grade commercially available.

Cloning and Expression of Cdc25B. The catalytic domain constructs Δ25B1 (residues 377−549) and Δ25B2 (residues 377−566) were constructed as follows. The primers gacagtgaccccatggagctgattgg (L1) and atcatcaagctttcactggtcctgcagc for Δ25B2, or L1 and gctcccaagcttagctgcgagtcttgaggc for Δ25B1, were used in a PCR amplification for 25 cycles with denaturation at 95 °C for 30 s, annealing at 55 °C for 30 s, and extension for 1 min at 72 °C. Following digestion with *Nco*I and *Hin*dIII, the PCR fragments were cloned into the *Nco*I and *Hin*dIII sites of the pET3C vector. The E474Q and E478Q mutants were generated using the Quick-Change method from Strategene using the following primers: ttccactgtCaattctcatctgagcgtgg and gatgagaattGacagtggaaaatgagg for E474Q and ctcatctCagcgtgggccccgcatgtgcc and cccacgctGagatgagaattcacagtgg for E478Q (mutated nucleotides are uppercase). The resulting plasmids were transformed into

Escherichia coli BL-21(DE3) cells, and single colonies were selected and grown in LB medium supplemented with 50 μg/mL ampicillin at room temperature. Protein expression was induced when the cells reached an OD_{600} of 0.6 by addition of isopropyl 1-thio-β-D-galactopyranoside to a final concentration of 0.5 mM. Following an additional 3 h of growth at room temperature, the cells were harvested by centrifugation at 4000*g* for 20 min and the cells were frozen in liquid nitrogen.

Purification of Cdc25B Proteins. All steps in the purification were performed at 4 °C, and phosphatase activity was followed by assays using pNPP as a substrate. In a typical preparation, 7 g of frozen cell pellets was thawed in 50 mL of buffer A [20 mM MES (pH 6.0), 1 mM EDTA, and 1 mM DTT] supplemented with Complete protease inhibitor cocktail from Boehringer Mannheim. The cells were lysed by sonication (three times, 30 s). Following centrifugation at 25000*g* for 30 min, the cleared lysate was bound to 7 mL of SP-Sepharose equilibrated in buffer A. Cdc25B was eluted with a gradient in buffer A to 0.5 M NaCl and further purified by S-200 chromatography in TNED buffer [50 mM Tris-HCl (pH 7.5), 50 mM NaCl, 1 mM EDTA, and 1 mM DTT]. The purified protein (>95% pure) was concentrated to 10 mg/mL in Ultrafree concentrators from Millipore and frozen in liquid N_2 for storage at −80 °C.

Preparation of Cdk2-pTpY/CycA. An N-terminal region of the Myt1 protein from *Xenopus laevis* (residues 1−372) was subcloned into the pGEX4T-1 expression vector using the *Eco*RI and *Not*I restriction sites. The resulting plasmid was transformed into *E. coli* BL-21(DE3) cells, and the GST-cat-Myt1 fusion protein was expressed as described above for Cdc25B. GST-cat-Myt1 was purified as described previously (J. Rudolph et al., submitted for publication). Cdk2-pTpY/CycA was prepared fresh each day starting with Cdk2/CycA (200 μg), GST-cat-Myt1 (60 μg), and [γ-^{32}P]ATP (3.3 mM, SA = 1−4 × 10^{14} cpm/mol) for 2 h in 50 mM Tris-HCl (pH 7.5), 50 mM NaCl, 10 mM $MgCl_2$, 1 mM DTT, and 0.05% Triton X-100. Following the phosphorylation reaction, GST-Myt1 bound to the GSH beads was removed by centrifugation at 1000*g* for 5 min. Unincorporated ATP was removed by G-50 chromatography (1 cm × 15 cm) in 20 mM HEPES (pH 7.5), 50 mM NaCl, and 5 mM DTT.

Assays. All phosphatase reactions were performed in a three-component buffer system (50 mM Tris, 50 mM Bis-Tris, and 100 mM sodium acetate) containing 1 mM DTT at 25 °C. Reactions using *p*-nitrophenyl phosphate (pNPP) and 3-*O*-methylfluorescein phosphate (mFP) were followed by continuous UV−vis spectroscopy at 410 nm (ϵ = 18 000 M^{-1} cm^{-1}) and 477 nm (ϵ = 27 200 M^{-1} cm^{-1}), respectively. Assays using mFP at enzyme concentrations of 1−5 nM contained 0.01% Tween 20 to prevent loss of enzyme activity. All assays using pNPP and mFP consisted of complete K_m determinations using more than eight concentrations of substrate between 0.2 and 5K_m, and the results were fitted to eq 1 using Cleland's programs (*21*) in the KinetAsyst package (IntelliKinetics).

$$v = [E]_0 k_{cat}[S]/([S] + K_m) \quad (1)$$

Reactions with the natural substrate Cdk2-pTpY/CycA were performed using 0.2−10 nM enzyme in the presence of 1 mg/mL bovine serum albumin and at fixed time points were quenched by the addition of 0.3 equiv (by volume) of 30% TCA. The supernatant containing the released phosphate was subjected to scintillation counting following centrifugation of the precipitated protein at 14 K and 4 °C for 10 min. Assays using Cdk2-pTpY/CycA were limited to k_{cat}/K_m determinations at 100−300 nM substrate because of the limiting amounts and concentrations of the substrate. Time dependence (five points minimum), substrate concentration dependence (two differing concentrations), and enzyme concentration dependence (two differing concentrations) were tested and ensured for each assay. The pH-dependent activities of the catalytic domains of Cdc25B were fitted to eqs 2−4 using IGOR software (Wavemetrics), as indicated in the results.

Scheme 2: Simplest Kinetic Mechanism of DSPs

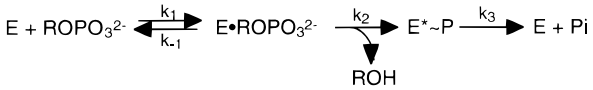

$$v = C/(1 + [H]/K_a) \quad (2)$$

$$v = C/(1 + [H]/K_a)(1 + [H]/K_b) \quad (3)$$

$$v = C/(1 + [H]/K_a + [H]/K_b + K_c/[H]) \quad (4)$$

In eqs 2−4, C is the pH-independent value of k_{cat} or k_{cat}/K_m, [H] is the proton concentration, and K_a, K_b, and K_c are three independent ionization constants. The pH range on the lower end of these experiments was limited to 5.25 because this was the lowest pH where incubation of Cdc25B led to recovery of activity upon dilution into assay buffer at pH 7.5. The rates of reaction were corrected for pH-dependent changes in the extinction coefficients of pNPP and mFP.

Rapid Reaction Kinetics. Burst experiments were performed using a Bio-Logic stop flow instrument by monitoring the formation of product at 410 nm (for the substrate pNPP) or 477 nm (for the substrate mFP) following a 13 ms mixing time in a 0.2 mm cuvette. Enzyme concentrations ranged from 1 to 5 μM and substrate concentrations of mFP from 31 to 500 μM, whereas the concentration of pNPP was fixed at 70 mM. The pH-dependent bursts using mFP were performed using the three-component buffer for both the enzyme and substrate solutions. The primary burst data were analyzed by fitting to eq 5 using IGOR software. The values for K_S (k_{-1}/k_1), k_2, and k_3 (see Scheme 2) were determined as described for burst experiments with chymotrypsin and relied on fitting to eqs 6 and 7 using IGOR software (*22*).

$$\text{product} = Ae^{-k_1 t} + k_2 t + c \quad (5)$$

$$\text{rate of burst} = (k_2 + k_3)[S]/([S] + K_S) \quad (6)$$

$$\text{burst} = [E]_0[k_2/(k_2 + k_3)]^2/(1 + K_m/[S])^2 \quad (7)$$

RESULTS

Protein Expression and Purification. Two different catalytic domain constructs were designed to study the pH-dependent behavior of Cdc25B. The first, Δ25B1, corresponds to the visible structure as determined by X-ray crystallography (*18*). Δ25B1 begins at the conserved LIGD motif originally identified as the beginning of the catalytic region (*23*) and ends 18 residues from the natural C-terminus

Table 1: Kinetic Parameters of Δ25B1 and Δ25B2 toward the Substrates pNPP, mFP, and Cdk2-pTpY/CycA at pH 6.5 and room temperature

enzyme	parameter	pNPP	mFP	Cdk2-pTpY/CycA
Δ25B1	K_m	13.8 ± 1.2 mM	25 ± 4 μM	nd[a]
	k_{cat}	0.170 ± 0.007 s^{-1}	2.3 ± 0.1 s^{-1}	nd[a]
	k_{cat}/K_m	12 ± 1.4 M^{-1} s^{-1}	95 000 ± 21 000 M^{-1} s^{-1}	178 000 ± 12 000 M^{-1} s^{-1}
	burst kinetics	no	yes (0.98 ± 0.05 equiv)	nd[a]
Δ25B2	K_m	10.5 ± 0.8 mM	51 ± 8.5 μM	nd[a]
	k_{cat}	0.162 ± 0.005 s^{-1}	2.8 ± 0.22 s^{-1}	nd[a]
	k_{cat}/K_m	15 ± 1.1 M^{-1} s^{-1}	54 000 ± 15 000 M^{-1} s^{-1}	1 300 000 ± 82 000 M^{-1} s^{-1}
	burst kinetics	no	yes (0.25 ± 0.02 equiv)	nd[a]

[a] Not determined.

of Cdc25B. Because Δ25B1 corresponds closely to the visible structure, it was used as the test protein to investigate the role of the potential catalytic acids. The other catalytic domain construct, Δ25B2, also begins at the LIGD motif but continues to the natural C-terminal end of the protein. This construct was made and subjected to selected assays to ensure that the C-terminal truncation of Δ25B1 did not yield any unexpected results and to investigate the role of the C-terminal tail in catalysis. Both Δ25B1 and Δ25B2 were expressed in *E. coli* and purified to >95% homogeneity as judged by SDS−PAGE and Coomassie staining with yields of 1−3 mg/L. The Δ25B1 and Δ25B2 proteins were monomeric as judged by S-200 chromatography and were stable to repeated freezing and thawing without loss of activity.

Initial Kinetic Characterization. The minimal kinetic scheme for reactions of PTPs and DSPs with their substrates has been well established by extensive enzymological studies for a number of representative enzymes (Scheme 2). The bis-anionic substrate binds to the free enzyme to form an ES complex (defined by k_1 and k_{-1}). The binding step includes a substrate-induced conformational change that brings the catalytic acid into position above the oxygen of the leaving group. The nucleophilic cysteine then attacks the phosphate and is accompanied by protonation of the leaving group by the catalytic acid (defined by k_2 and assumed to be irreversible). The covalent phosphorylated enzyme is subsequently hydrolyzed by water to yield inorganic phosphate and free enzyme (defined by k_3 and assumed to be irreversible). In terms of kinetic analyses, the second-order rate constant k_{cat}/K_m describes the kinetic events between the free enzyme and free substrate, from substrate binding up to and including the first irreversible step, namely, the loss of the leaving group. On the other hand, the rate constant k_{cat} describes the rate-limiting events of the overall reaction. In this report, the k_{cat}/K_m and k_{cat} parameters were evaluated in a pH-dependent manner for a number of substrates of the Cdc25 phosphatase to determine the identities and roles of the key catalytic residues in this enzyme.

The artificial substrate pNPP is most commonly used to assay PTPs and DSPs. As has been noted previously, pNPP is a rather poor substrate for the Cd25s (*24*, *25*). The k_{cat} and k_{cat}/K_m of pNPP toward Δ25B1 were found to be 0.17 s^{-1} and 12.3 M^{-1} s^{-1}, respectively, at pH 7.5 and room temperature (Table 1). The Δ25B2 construct displayed essentially the same kinetic parameters (k_{cat} = 0.16 s^{-1} and k_{cat}/K_m = 8.6 M^{-1} s^{-1}). These results are in reasonable agreement with those measured previously for a catalytic domain of Cdc25B derived from a GST fusion protein and encompassing essentially the same residues (378−566) (*26*). These results are also consistent with the results obtained in proteolytic truncation experiments where loss of the last 22 residues of Cdc25B had no effect on the K_m of pNPP (*18*) and confirm that the region of Cdc25B corresponding to the visible structure from crystallography is catalytically competent. In one-turnover experiments, no burst is seen for the reaction of either Δ25B2 or Δ25B1 with pNPP, suggesting that the rate-determining step in the reaction occurs prior to or during initial product formation (Table 1). Also, the addition of a 3-fold excess of unphosphorylated Cdk2/CycA, the product of a natural substrate of Cdc25B, had no effect on the k_{cat} or k_{cat}/K_m for pNPP at pH 7.0.

As has been noted previously, mFP is a much better substrate for the Cdc25 phosphatases than pNPP (*26*). The k_{cat} and k_{cat}/K_m of mFP toward Δ25B1 were found to be 2.4 s^{-1} and 95 000 M^{-1} s^{-1}, respectively (Table 1), again in reasonable agreement with these previous results. Similar kinetic parameters were obtained for the longer catalytic domain, Δ25B2 (2.8 s^{-1} and 54 000 M^{-1} s^{-1} for k_{cat} and k_{cat}/K_m, respectively). In one-turnover experiments, a burst of 0.98 equiv is seen for the reaction of Δ25B1 with mFP (Table 1). The observed burst supports the usual two-step reaction mechanism that is a characteristic of PTPs and DSPs with formation of a phosphocysteine intermediate as shown in Scheme 1. The observed burst with mFP also emphasizes the different reactivities of these two artificial substrates. The reaction with pNPP has a rate-determining step in the first half-reaction, whereas the reaction with mFP has the hydrolysis of the phosphoenzyme intermediate as its rate-determining step.

Recently, the availability of sufficient well-characterized quantities of Cdk2-pTpY/CycA has allowed the determination of the kinetic parameters of Cdc25 for a natural substrate (J. Rudolph et al., submitted for publication). These authors have shown that Cdc25 is an amazingly fast and efficient enzyme when presented with a natural substrate. The Δ25B1 and Δ25B2 constructs were tested using the Cdk2-pTpY/CycA substrate and were found to be 14000- and 86000-fold more potent as a substrate than pNPP, respectively (Table 1), in agreement with the previous results. Minimal catalytic domains of the Cdc25s, as represented by Δ25B1, are thus catalytically competent both with artificial and especially with natural substrates.

pH Dependence of Δ25B1. We began our search for the catalytic acid in the Cdc25 reaction mechanism by performing pH-dependent assays with the substrate pNPP. Interestingly, the pH dependence of the Cdc25B reaction toward pNPP for neither k_{cat} nor k_{cat}/K_m corresponds to the typical bell-shaped profile seen for other DSPs and PTPs (Figure 1). Although one does observe a pH dependence between

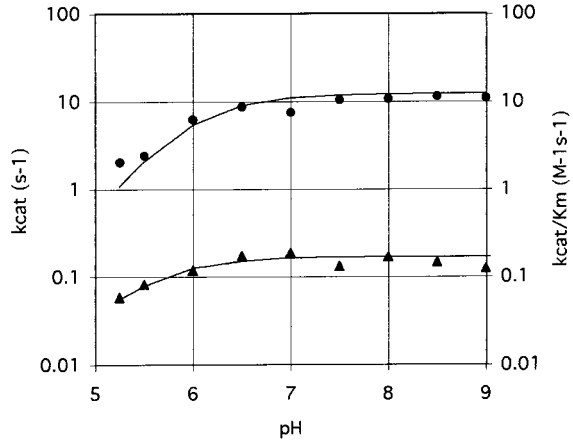

FIGURE 1: pH−rate profile of k_{cat} (▲) and k_{cat}/K_m (●) for Δ25B1 with the substrate pNPP.

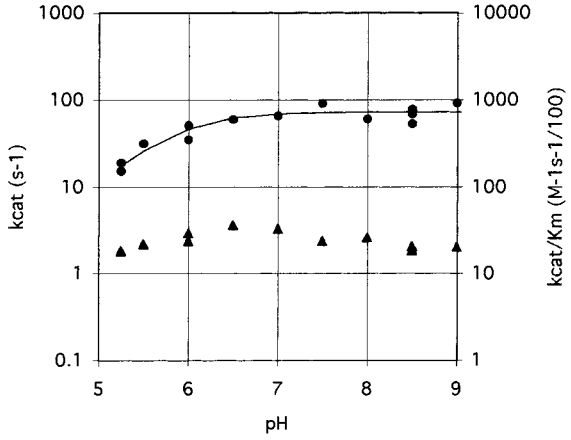

FIGURE 2: pH−rate profile of k_{cat} (▲) and k_{cat}/K_m (●) for Δ25B1 with the substrate mFP.

pH 5.25 and 7 using the Δ25B1 construct, there is no apparent pH dependence for this reaction between pH 7 and 9 for either k_{cat}/K_m or k_{cat}. The data for the pH dependence of k_{cat}/K_m were fitted to eq 3 containing two groups that need to be deprotonated for maximal activity and are more than 0.5 pH unit apart. This fitting procedure was facilitated by fixing the pK_a for the dianionic pNPP at pH 5.1 (*27*), a procedure made necessary by the instability of Δ25B1 to reaction conditions below pH 5.25. The other pK_a was then found to be 6.1 (Table 2) and, on the basis of the precedence from other PTPs and DSPs, most likely corresponds to the ionization state of the catalytic cysteine nucleophile. The data for the pH dependence of the k_{cat} of pNPP were fitted to eq 2 containing only one pK_a. The observed pK_a of 5.6 was assigned to the catalytic cysteine nucleophile. These results are consistent with the characterization of pNPP as a poor substrate. Under k_{cat}/K_m conditions, both substrate binding and phosphate transfer are partially rate-determining, whereas under k_{cat} conditions, where the substrate is present in saturating amounts, only the pH dependence of the formation of the phosphocysteine intermediate is observed. The lack of a basic limb (between pH 6.5 and 9) in the pH dependence suggests either that Cdc25B does not employ a catalytic acid or that the effect of the catalytic acid is kinetically masked in both the binding and catalysis steps of the reaction of pNPP with Cdc25B. Given the relatively slow rate of reaction of Cdc25 with pNPP, especially in comparison to other DSPs that have 10^4-10^5-fold higher k_{cat}/K_m values for pNPP (*28*), the possibility that the Cdc25 phosphatases do not employ a catalytic acid is not an unreasonable suggestion.

Since the reaction of Cdc25 with mFP has a different rate-determining step, we thought this may be a useful tool for elucidating the catalytic acid of Cdc25B. However, the pH dependence of Cdc25B toward mFP as measured by k_{cat} or k_{cat}/K_m also does not generate the bell curve expected from the precedence of other PTPs and DSPs (Figure 2). Indeed, the profiles are almost completely flat, especially for the k_{cat} versus pH data that could not be fitted satisfactorily. The k_{cat}/K_m data were fitted to eq 2 to yield an apparent pK_a of 5.8 (Table 2). Thus, under k_{cat}/K_m conditions where substrate is limiting, one can detect the role of the catalytic cysteine in the chemical reaction. We do not observe the ionization state of mFP under k_{cat}/K_m conditions, presumably because of the high commitment to catalysis displayed by this enzyme wherein $K_s \gg K_m$ and $k_2 \gg k_{-1}$ (see one-turnover kinetics below). On the other hand, under k_{cat} conditions, the rate-determining step becomes breakdown of the phosphocysteine intermediate that requires neither a negatively charged substrate nor an anionic cysteine and therefore exhibits no pH dependence at all.

To confirm the assignment of the observed pK_a of 5.6−5.8 to the catalytic cysteine residue in Cdc25B, we determined the pH dependence of the burst kinetics with mFP. By performing rapid reaction kinetics at varying concentrations of the substrate mFP, one can determine the values for K_S (k_{-1}/k_1), k_2, and k_3 as defined in Scheme 2. Typical results from monitoring product formation at pH 6.5 that were fit to eq 5 are shown in Figure 3A. By fitting the rates of burst formation and burst amplitudes at varying substrate concentrations and varying pH's to Equations 6 and 7 (as shown for pH 6.5 in Figure 3B), we determined k_2, the actual pH-independent rate constant representing phosphate transfer from substrate to enzyme in Scheme 2 (Table 3). Figure 3C shows the results of plotting the resulting k_2 values versus pH, which was fitted to eq 2 to yield a pK_a of 6.3. In summary, the steady-state experiments and the burst experiments verify a range of 5.6−6.3 for the pK_a of the catalytic cysteine in Cdc25B and justify the assumption of a pK_a of 5.9 in the curve fitting for the assays utilizing the natural substrate Cdk2-pTpY/CycA (see below).

Table 2: Fitting Parameters (pK_as and pH-independent k_{cat} or k_{cat}/K_m values) from the Δ25B1-Catalyzed Reaction with the Substrates pNPP and mFP[a]

parameter	pNPP (k_{cat})	pNPP (k_{cat}/K_m)	mFP (k_{cat}/K_m)	mFP burst (k_2)
pK_a(substrate)	−	*5.1*	−	−
pK_a(Cys473)	5.6 ± 0.2	6.1 ± 0.3	5.7 ± 0.2	6.3 ± 0.3
pH-independent constant	0.17 ± 0.01 s^{-1}	12.3 ± 0.1 M^{-1} s^{-1}	72 600 ± 4200 M^{-1} s^{-1}	211 ± 17 s^{-1}

[a] All assays were performed in three-component buffer at room temperature, and the pK_as were determined by fitting to the appropriate equation as described in the text. The italic value was fixed in the fitting procedure as described in the text.

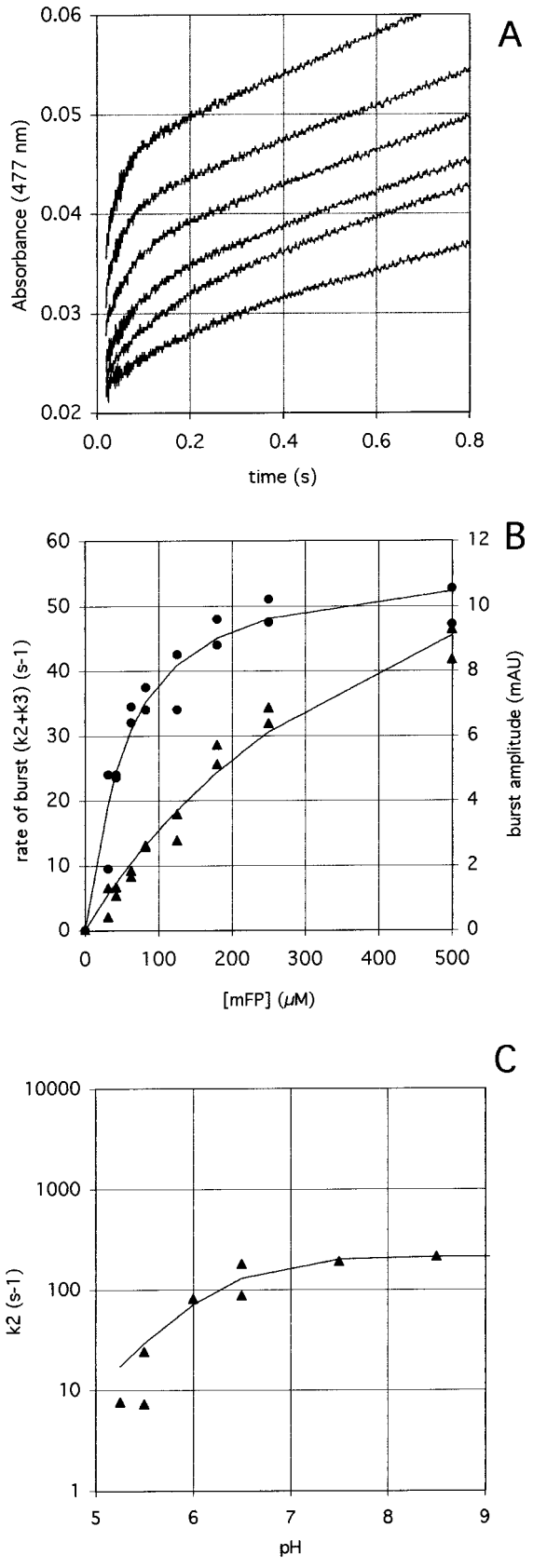

FIGURE 3: (A) Typical mFP bursts results at pH 6.5 and varying mFP concentrations (from top to bottom, 250, 180, 125, 82, 62, and 42 μM). (B) Substrate dependence vs the rate of burst (▲) and burst amplitude at pH 6.5 (●) as fitted to eqs 6 and 7, respectively. (C) pH−rate profile of k_2 for Δ25B1 with the substrate mFP as derived from the burst experiments.

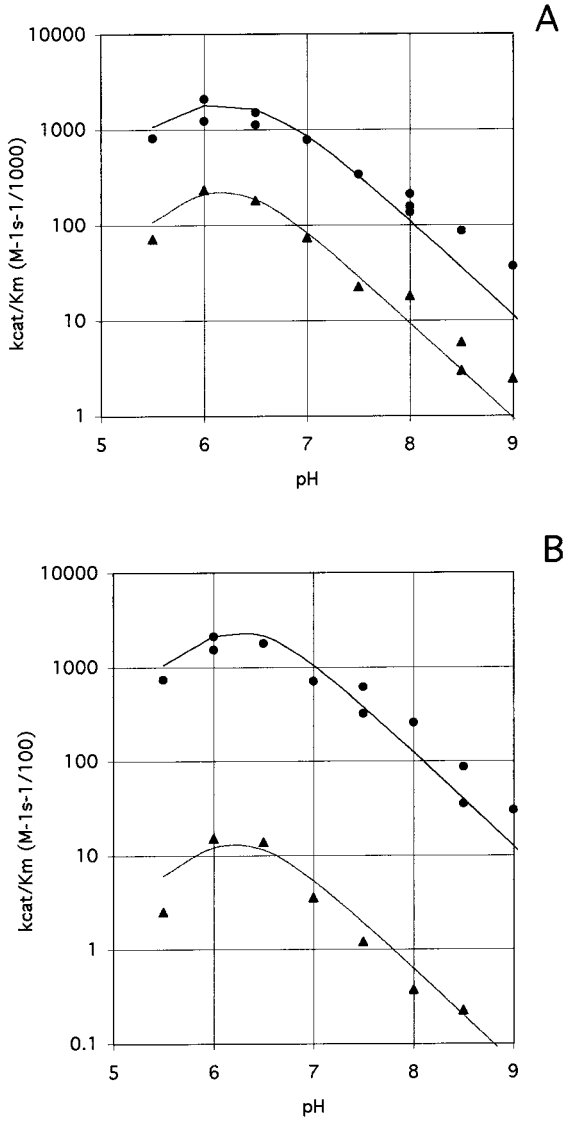

FIGURE 4: (A) pH−rate profile of k_{cat}/K_m for Δ25B1 (▲) and Δ25B2 (●) with the substrate Cdk2-pTpY/CycA. (B) pH−rate profile of k_{cat}/K_m for E474Q (▲) and E478Q (●) with the substrate Cdk2-pTpY/CycA.

Table 3: Fitting Parameters from the Rapid Reaction Kinetics Performed with mFP Obtained from eqs 5−7

pH	k_2 (s^{-1})	k_3 (s^{-1})	K_S (μM)	K_m (μM)
5.25	7.6 ± 2.0	4.4 ± 1.50	47 ± 25	200 ± 49
5.5	24 ± 11	1.7 ± 0.55	320 ± 200	71 ± 35
6	180 ± 61	1.9 ± 0.28	810 ± 350	29 ± 5.2
6.5	87 ± 10	1.6 ± 0.20	480 ± 90	17 ± 2.4
7.5	190 ± 47	1.7 ± 0.28	840 ± 340	15 ± 2.3
8.5	213 ± 71	1.9 ± 0.19	940 ± 270	13 ± 2.9

When the pH dependence of Cdc25B toward the natural substrate Cdk2-pTpY/CycA was assayed (k_{cat}/K_m), the bell-shaped curve expected for an enzyme of the DSP family was finally observed (Figure 4A). Radiolabeled Cdk2-pTpY/CycA was prepared by Myt1 phosphorylation of Cdk2/CycA in the presence of [γ-^{32}P]ATP and used to monitor the Δ25B1-catalyzed loss of phosphothreonine from the bis-phosphorylated complex (J. Rudolph et al., submitted for publication). Fitting of the data for the k_{cat}/K_m to eq 4 was facilitated by fixing the pK_a of the catalytic cysteine at 5.9 and the pK_a of the phosphothreonine substrate at pH 6.0 (*29*,

Table 4: Fitting Parameters for Various Forms of Cdc25B Using the Natural Substrate Cdk2-pTpY/CycA As Derived Using eq 4[a]

parameter	Δ25B1 (k_{cat}/K_m)	Δ25B1 (k_{cat}/K_m)	E474Q (k_{cat}/K_m)	E478Q (k_{cat}/K_m)
pK_a(catalytic acid)	6.1 ± 0.2	6.1 ± 0.3	6.2 ± 0.3	6.3 ± 0.2
pH-independent constant	750 000 ± 76 000 M^{-1} s^{-1}	9 100 000 ± 320 000 M^{-1} s^{-1}	42 000 ± 8400 M^{-1} s^{-1}	720 000 ± 71 000 M^{-1} s^{-1}

[a] The pK_a of the substrate was fixed at 6.0, and the pK_a of Cys473 was fixed at 5.9.

30). This procedure yielded an apparent pK_a of 6.2 for the catalytic acid, entirely consistent with the determination of ionization constants for catalytic acids in other DSPs [i.e., Asp92 in VHR with a pK_a of 5.7 (*31*)]. An identical pH profile was seen for the longer Δ25B2 construct (Figure 4A), thus ruling out the involvement of the 17 C-terminal residues in this effect. Thus, it appears that the Cdc25B reaction with its natural substrate does indeed require a catalytic acid and that this catalytic acid should be found in the minimal structure as visualized by crystallography.

Potential Catalytic Acids. Having observed a pH dependence in the basic limb of the Cdc25B reaction with the natural substrate Cdk2-pTpY/CycA, we set out to determine whether this effect was due to one of the two glutamates recently proposed to play such a role (*17*, *18*). We addressed these questions by constructing, expressing, and purifying the E474Q and E478Q mutants of Δ25B1. Both of these proteins were expressed well and were purified to homogeneity using the same protocol as for the wild-type protein. Surprisingly, given that these residues are located in the critical active site loop of Cdc25 and are highly conserved, their mutation to Gln at first glance caused no effect on the overall activity of Cdc25 toward pNPP. The specific activities of the E474Q and E478Q mutant enzymes toward pNPP at pH 7.5 were found to be 0.41 and 0.42 μmol min^{-1} mg^{-1}, respectively, compared to 0.39 μmol min^{-1} mg^{-1} for the wild-type protein. Additionally, the pH−rate profiles with pNPP (k_{cat} and k_{cat}/K_m) were identical to the that of the wild-type enzyme, namely, without the bell-shaped profile (data not shown). When the k_{cat}/K_m for Cdk2-pTpY/CycA with the mutants was measured, two interesting observations were made (Figure 4B and Table 4). First, the bell-shaped profile characteristic of the wild-type enzyme is retained for both mutants. This means that neither E474 nor E478 is the elusive catalytic acid of Cdc25B. Second, the overall activity of E474Q is 100-fold lower than the wild-type activity, whereas E478Q had the same activity toward Cdk2-pTpY/CycA. This is particularly interesting in that both mutants had identical specific activities against the artificial substrate pNPP.

DISCUSSION

In this paper, we have shown that Cdc25 appears to behave like other well-characterized DSPs. We have shown the pK_a of the catalytic cysteine to be 5.6−6.3, similar to those of other DSPs, by three different methods (pH-dependent activity with pNPP and mFP and burst kinetics). Cys124 in VHR, for example, was found to have a pK_a of 5.6 by IAA inactivation (*14*), whereas Cys403 in the *Yersinia* phosphatase has a pK_a of 4.67 (*8*). The low pK_as of the catalytic cysteines in phosphatases containing the HCX_5R motif have been attributed to either the histidine residue of the motif or the Ser/Thr residue often found immediately following the arginine residue of the motif. Interestingly, the Cdc25s do not contain a residue corresponding to an activating Ser/Thr residue, and His472 of Cdc25B is directed away from the active site. There are only two discernible reasons for the perturbed pK_a of Cys473 as seen in the crystal structures of Cdc25A and Cdc25B. First, Cys473 is strategically located above the following α-helix, which may give it a partially positively charged environment. Second, C473 appears to form a close interaction (2 Å) with the backbone NH of Gly480.

In addition to characterizing the catalytic cysteine, we have shown that the presence of a catalytic acid is indicated in the reaction of Cdc25 with the natural substrate. From a biophysical perspective, a catalytic acid appears to be a prerequisite in the phosphatase mechanism (Scheme 1). However, the combination of the slow reaction rate of Cdc25 toward artificial substrates (the k_{cat}/K_m of Δ25B1 toward pNPP is 2−3 orders of magnitude lower than those found for other DSPs) and the lack of pH dependence using these substrates raise the possibility that a catalytic acid is not involved in these reactions. While the pK_as of the leaving groups of pNPP and mFP (7.14 and 4.5, respectively) may favor the Cdc25 reaction proceeding without a catalytic acid, the pK_as of the threonyl- and tyrosyl-leaving groups of the substrate Cdk2-pTpY are significantly less favorable (∼18 and ∼10, respectively). These pK_as emphasize the necessity of a catalytic acid in the reaction mechanism of Cdc25 and are borne out by the observed pH dependence at pH >7.0 in the reaction of Cdc25 with Cdk2-pTpY/CycA, thus favoring the existence of a catalytic acid.

Upon examination of the two available structures of catalytic domains of Cdc25, however, no residue appears to be ideally situated to play the role of the catalytic acid. PTPs and DSPs with known structures all show a catalytic acid on a loop overhanging the active site. For example, in the *Yersinia* PTP, the catalytic acid (Asp356) is located on a loop that has been found in both open and closed conformations, depending on the occupancy of the active site (*11*, *32*, *33*). In the structure determined with the covalent inhibitor vanadate, the apical oxygen of the inhibitor forms a hydrogen bond to Asp356, consistent with its role as the catalytic acid. In the structure of VHR, the catalytic acid (Asp121) also overhangs the active site on a separate loop, although it is positioned on the opposite side of the active site compared to the *Yersinia* structure (*15*). No analogous loop can be found in the Cdc25 structures. The only two acidic residues located anywhere in the vicinity of the active site that could play the role of the catalytic acid are E474 and E478 in Cdc25B (corresponding to Glu431 and Glu435 in Cdc25A). Given the lack of a dianion in the structure of the catalytic domain of Cdc25A, it is difficult to make any conclusive predictions about the distance that either Glu431 or Glu435 would be away from the leaving group. In the structure of the catalytic domain of Cdc25B, either Glu474 or Glu478 appears to be close enough to interact with the apical oxygen of the sulfate, although the proposed catalytic

acid Glu474 is held away from the phosphate-binding region by three hydrogen bonds. Given the lack of any other possible residues, it is not unreasonable to speculate that Glu474 or Glu478 could play the role of the catalytic acid in Cdc25B. Also, we considered the possibility that the 17 C-terminal amino acids of the catalytic domain of Cdc25B (or 31 residues of Cdc25A), which are disordered in the crystal structure(s), could organize upon substrate binding to bring one of the two highly conserved glutamates of the C-terminus (Glu553 and Glu558 in Cdc25B) into the proximity of the active site.

Our mutagenesis results demonstrate that the catalytic acid is not located in the C-terminal region of the protein, nor is it Glu474 nor Glu478. Interestingly, although both the E474Q and E478Q mutants had activities identical to that of the wild-type protein in assays with pNPP, the E474Q mutant was 100-fold less active toward the Cdk2-pTpY/CycA. Consistent with its prominent role in catalysis with the natural substrate, Glu474 is also 100% conserved in all known Cdc25s, whereas an acidic residue corresponding to Glu478 is absent in organisms ranging from yeast to *Caenorhabditis elegans*. As mentioned in the introductory section, Glu474 forms hydrogen bonds to a number of residues around the active site and may be crucial in creating a suitable recognition site for the Cdk2-pTpY/CycA substrate.

The mitogen-activated protein kinase phosphatase (MKP3) is a DSP that for a time appeared to lack a catalytic acid in its reaction with pNPP (*34*). The structure of the catalytic domain of MKP3 has been determined recently with a chloride ion bound in the active site and shows a distorted active site reminiscent of the active site of Cdc25 (*12*). The HCX_5R motif, in particular, the arginine residue, is not optimally oriented to hold a dianionic substrate. Also, the loop containing the putative catalytic acid (Asp262) was seen in the open position, almost 5.5 Å away from the equivalent position in VHR. Interestingly, these authors also demonstrated that the nonphosphorylated substrate, extracellular signal-regulated kinase (ERK2), could activate MKP3 by a mechanism dependent on the presence of Asp262. The mechanism of this activation has recently been elucidated in pH-dependent, steady-state, and pre-steady-state kinetics experiments (*35*, *36*). Basically, binding of the substrate induces closure of the loop containing Asp262 such that this catalytic acid is in the correct position to contribute to the catalytic potential of the enzyme. This substrate-induced conformational change could be mimicked by the addition of either glycerol to a final concentration of 50% or DMSO to 30%. Although uncertain which residue could play the role of the catalytic acid, we tested whether a similar mechanism could apply to Cdc25 by measuring the k_{cat}/K_m of pNPP for Δ25B1 at pH 7 in the presence of a 3-fold excess of unphosphorylated Cdk2/CycA. No significant changes in the kinetic parameters were seen, consistent with the lack of an observable loop on Cdc25 that could undergo such a conformational change.

In conclusion, we have presented evidence that the Cdc25 reaction with the natural substrate requires all of the elements associated with members of the DSP family. It requires a catalytic cysteine, in the deprotonated state with a pK_a of 5.9, and requires binding of a dianionic substrate. Importantly, upon dephosphorylation of the natural substrate Cdk2-pTpY/CycA, it requires the function of a catalytic acid with a pK_a of 6.1. We have tested the hypotheses presented by the crystallographers that Glu474 or Glu478 in Cdc25B could play the role of the catalytic acid and found that this is not the case. Additionally, we have determined that the catalytic acid is not located in the unstructured C-terminal region of the catalytic domain of Cdc25. Thus, by deductive reasoning, we propose that the catalytic acid may be located on the substrate Cdk2-pTpY/CycA. This would provide a dramatic example of how nature has ensured for exquisite substrate specificity among the ubiquitous and potentially promiscuous protein phosphatases. Experiments are underway to test this hypothesis and determine the actual identity of this key catalytic residue.

REFERENCES

1. Barford, D., Das, A. K., and Egloff, M. P. (1998) *Annu. Rev. Biophys. Biomol. Struct. 27*, 133−164.
2. Nilsson, I., and Hoffman, I. (2000) *Prog. Cell Cycle Res. 4*, 107−114.
3. Galaktionov, K., and Beach, D. (1991) *Cell 67*, 1181−1194.
4. Denu, J. M., Stuckey, J. A., Saper, M. A., and Dixon, J. E. (1996) *Cell 87*, 361−364.
5. Denu, J. M., Lohse, D. L., Vijayalakshmi, J., Saper, M. A., and Dixon, J. E. (1996) *Proc. Natl. Acad. Sci. U.S.A. 93*, 2493−2498.
6. Zhang, Z.-Y. (1995) *J. Biol. Chem. 270*, 11199−11204.
7. Jia, Z., Barford, D., Flint, A. J., and Tonks, N. (1995) *Science 268*, 1754−1758.
8. Zhang, Z. Y., and Dixon, J. E. (1993) *Biochemistry 32*, 9340−9345.
9. Zhang, Z.-Y., Wang, Y., and Dixon, J. E. (1994) *Proc. Natl. Acad. Sci. U.S.A. 91*, 1624−1627.
10. Flint, A. J., Tiganis, T., Barford, D., and Tonks, N. K. (1997) *Proc. Natl. Acad. Sci. U.S.A. 94*, 1680−1685.
11. Stuckey, J. A., Schubert, H. L., Fauman, E. B., Zhang, Z.-Y., Dixon, J. E., and Saper, M. A. (1994) *Nature 370*, 571−575.
12. Stewart, A. E., Dowd, S., Keyse, S., and McDonald, N. Q. (1999) *Nat. Struct. Biol. 6*, 174−181.
13. Wu, L., and Zhang, Z.-Y. (1996) *Biochemistry 35*, 5426−5434.
14. Denu, J. M., Zhou, G., Wu, L., Zhao, R., Yuvaniyama, J., Saper, M. A., and Dixon, J. E. (1995) *J. Biol. Chem. 270*, 3796−3803.
15. Yuvaniyama, J., Denu, J. M., Dixon, J. E., and Saper, M. A. (1996) *Science 272*, 1328−1331.
16. Zhao, G., Denu, J. M., Wu, L., and Dixon, J. E. (1994) *J. Biol. Chem. 269*, 28084−28090.
17. Fauman, E. B., Cogswell, J. P., Lovejoy, B., Rocque, W. J., Holmes, W., Montana, V. G., Piwnica-Worms, H., Rink, M. J., and Saper, M. A. (1998) *Cell 93*, 617−625.
18. Reynolds, R. A., Yem, A. W., Wolfe, C. L., Deibel, M. R. J., Chidester, C. G., and Watenpaugh, K. D. (1999) *J. Mol. Biol. 293*, 559−568.
19. Hofmann, K., Bucher, P., and Kajava, A. V. (1998) *J. Mol. Biol. 282*, 195−208.
20. Eckstein, J. W., Beer-Romero, P., and Berdo, I. (1996) *Protein Sci. 5*, 5−12.
21. Cleland, W. W. (1979) *Methods Enzymol. 63*, 103−138.
22. Bender, M. L., Kezdy, F. J., and Wedler, F. C. (1967) *J. Chem. Educ. 44*, 84−88.
23. Xu, X., and Burke, S. P. (1996) *J. Biol. Chem. 271*, 5118−5124.
24. Dunphy, W. G., and Kumagai, A. (1991) *Cell 67*, 189−196.
25. Millar, J. B. A., Blevitt, J., Gerace, L., Sadhu, K., Featherstone, C., and Russell, P. (1991) *Proc. Natl. Acad. Sci. U.S.A. 88*, 10500−10504.
26. Gottlin, E., Epstein, D. M., Eckstein, J., and Dixon, J. (1996) *J. Biol. Chem. 272*, 27445−27449.
27. Zhang, Z.-Y., Malachowski, W. P., Van Etten, R., and Dixon, J. E. (1994) *J. Biol. Chem. 269*, 8140−8145.

28. Chen, L., Montserat, J., Lawrence, D. S., and Zhang, Z.-Y. (1996) *Biochemistry 35*, 9349−9354.
29. Charifson, P. S., Shewchuk, L. M., Rocque, W., Hummel, C. W., Jordan, S. R., Mohr, C., Pacofsky, G. J., Peel, M. R., Rodriguez, M., Sternbach, D. D., and Consler, T. G. (1997) *Biochemistry 36*, 6283−6293.
30. Schutkowski, M., Bernhardt, A., Zhou, X. Z., Shen, M., Reimer, U., Rahfeld, J.-U., Lu, K. P., and Fischer, G. (1998) *Biochemistry 37*, 5566−5575.
31. Denu, J. M., Zhou, G., and Dixon, J. E. (1995) *Biochemistry 34*, 3396−3403.
32. Fauman, E. B., Yuvaniyama, C., Schubert, H. L., Stuckey, J. A., and Saper, M. A. (1996) *J. Biol. Chem. 271*, 18780−18788.
33. Schubert, H. L., Fauman, E. B., Stuckey, J. A., Dixon, J. E., and Saper, M. A. (1995) *Protein Sci. 4*, 1904−1913.
34. Wiland, A. M., Denu, J. M., Mourey, R. J., and Dixon, J. E. (1996) *J. Biol. Chem. 271*, 33486−33492.
35. Zhou, B., and Zhang, Z. Y. (1999) *J. Biol. Chem. 274*, 35526−35534.
36. Fjeld, C. C., Rice, A. E., Kim, Y., Gee, K., and Denu, J. M. (2000) *J. Biol. Chem. 275*, 6749−6757.

BI000909U